Desalination and Water Treatment
www.deswater.com
doi: 10.1080/19443994.2013.855677

53 (2015) 1204–1212
February

Taylor & Francis
Taylor & Francis Group

Preparation of low-cost microfiltration membranes from fly ash

Gurpreet Singh, Vijaya Kumar Bulasara*

Department of Chemical Engineering, Thapar University, Patiala 147004, Punjab, India
Tel. +91 8437166806; Fax: +91 175 2393005; email: vkbulasara@thapar.edu

Received 11 August 2013; Accepted 2 October 2013

ABSTRACT

Commercial ceramic membranes have undergone a rapid growth during the last two decades. The interest in ceramic membranes has increased concurrently with new processes and applications. The development of membrane processes to treat wastewater is generally limited as the membranes especially the inorganic ones are highly expensive. The present work deals with the fabrication and characterization of ceramic membranes using cheaper raw materials. Disk type ceramic membranes were prepared using fly ash as the major constituent without using any polymeric additives. The membranes were sintered at four different temperatures (800, 850, 900 and 1,000˚C) to study the effect of sintering temperature on membrane properties. The membranes were characterized by thermo-gravimetric analysis, scanning electron microscopy and X-ray diffraction techniques and the porosity was determined gravimetrically. The prepared membranes had a porosity of 35–40%, average pore size of 1.2–2.3 μm and exhibited very good chemical stability in acidic as well as basic solutions. The SEM pictures indicated that the membranes were defect-free. The pure water permeability of the membranes varied from 1,234 to 5,566 L/(m^2 h bar). In comparison with other membranes, the membranes sintered at 900˚C had a uniform pore size distribution with an average pore diameter of 1.2 μm. Flux decline profiles for the separation of oil-in-water were obtained and maximum oil rejection of 99.2% was obtained for the membrane sintered at 900˚C which indicates that the membranes made of fly ash are useful for microfiltration applications.

Keywords: Fly ash; Low cost; Ceramic membrane; Microfiltration; Sintering temperature

1. Introduction

In the past two decades, considerable efforts have been made to reduce energy demands. The use of membrane technology to replace a separation or purification step in an industrial process may reduce the overall consumption of energy. Depending upon the size of particles to be retained, the pressure-driven processes namely microfiltration, ultrafiltration, nanofiltration and reverse osmosis are used [1]. Among these membrane-separation processes, the microfiltration and ultrafiltration are considered as critical technologies because of their low cost as they operate at low pressures. Membrane technology is continuously going through the advancement phase in the development of membranes that can be used in a wide variety of applications, keeping in mind the cost implications. Existing and continuing research in membrane technology aims at the fabrication of ceramic membranes that are suitable for high temperature applications [2] and corrosive feed stocks [3].

---

*Corresponding author.

Early research on inorganic membrane fabrication was focused towards the utilization of α-alumina [4], γ-alumina [5], zirconia [6], titania [3] and silica [2]. Since the cost of all these raw materials remains significantly high, there is a need to develop ceramic membranes from cheaper raw materials such as apatite powder [7], fly ash [8], natural raw clay [9–11], dolomite and kaolin [12]. Potdar et al. [13] and Neelakandan et al. [14] used kaolin, ball clay, quartz, feldspar, calcium carbonate and pyrophyllite for the fabrication of microfiltration range inorganic membranes. Of these precursors, quartz, feldspar and pyrophyllite fall into the category of expensive materials. One of the challenges in the development of inorganic membranes is to produce low-cost membranes from natural materials such as clay, fly ash and apatite which are in abundance and which need lower firing temperatures than metal oxide materials and have high flux performance to treat large volumes of liquid effluent. Few literatures were also found for the fabrication of membrane supports using mixture of clays [15]. Some studies indicate that the low-cost ceramic membranes could act as supports for ultrafiltration membranes [11,16].

In recent years, efforts have been made to use coal fly ash, a by-product of coal combustion in thermal power plants, for preparing low-cost ceramic membranes due to its high percentage of alumina and silica. Indeed, this allows a good management of this sub-product which represents a major problem in many parts of the world due to the resulting pollution. Jedidi et al. [17] used fly ash along with organic additives such as amijel (pregelated starch) and methocel (cellulose derivative) to prepare microfiltration ceramic membranes for treating dyeing effluent. As a very little research has been done to effectively use fly ash as a material for preparation of low-cost microfiltration membranes, its true potential is yet to be realized.

The present work is aimed at developing low-cost microfiltration ceramic membranes using fly ash along with inorganic materials like calcium carbonate, sodium metasilicate and boric acid. The idea behind this work was to develop a suitable composition based on fly ash that could be sintered at a temperature below 1,000˚C to reduce the processing cost of membrane.

2. Experimental methodology

2.1. Raw materials

Fly ash and four other inorganic raw materials namely calcium carbonate, sodium carbonate, boric acid and sodium metasilicate were used in this work to prepare low-cost ceramic membranes. Different raw materials used for fabricating membranes serve different purposes. Fly ash was chosen as its physicochemical characteristics, such as particle size and porosity, make it suitable for ceramic membrane fabrication. Sodium carbonate and boric acid act as colloidal agents for improving the dispersion properties of the raw material paste and creating homogeneity. Boric acid also forms metallic metaborates leading to improvement in the mechanical strength of membrane. Sodium metasilicate acts as binder by creating silicate bonds inducing higher mechanical strength [10,16]. Calcium carbonate under sintering conditions dissociates into CaO and CO_2 gas. The vacant space created by the release of CO_2 gas imparts porous structure to the membrane contributing to membrane porosity [18].

All chemicals (sodium carbonate, calcium carbonate, boric acid and sodium metasilicate) except fly ash were obtained from CDH India. Fly ash was obtained from Bathinda thermal power plant. Sodium carbonate, calcium carbonate, boric acid and sodium metasilicate were graded at least 99.5% pure and therefore, all of them were used without any pre-treatment. On the other hand, fly ash was heated to 550˚C and kept at this temperature for 4 h to remove any un-burnt carbon and volatile organic impurities. After this treatment, the colour of fly ash changed from light grey to tan.

2.2. Membrane preparation

The membrane fabrication process involved thorough mixing and grinding of raw materials like fly ash, sodium carbonate, sodium metasilicate, calcium carbonate and boric acid in a ball mill for 30 min. Composition of raw materials used for membrane fabrication on both dry basis and wet basis is given in Table 1. Grinding of raw materials was followed by paste preparation with the addition of distilled water. The paste was then casted in a circular ring of diameter 55 mm and thickness 5 mm. After this step, casted membrane disks were placed under distributed load of 2 kg for 12 h to prevent deformation and drive homogeneity which was followed by drying at room temperature. Then, the casted membranes were heated to 100˚C in a muffle furnace and kept there for about 12 h. After this, the temperature of the furnace was raised to 250˚C maintaining a heating rate of 50˚C/h and the membranes were heated for about 2 h at 250˚C. Again, the furnace temperature was increased up to the desired sintering temperature at a heating rate of 100˚C/h. Four sintering

Table 1
Composition of raw materials used for membrane fabrication

Material	Composition on dry basis (wt.%)	Composition on wet basis (wt.%)
Fly ash	65	50.0
Calcium carbonate	20	15.38
Sodium carbonate	10	7.69
Boric acid	2.5	1.92
Sodium metasilicate	2.5	1.92
Water	–	23.08

temperatures (800, 850, 900 and 1,000˚C) were used in this work to study the effect of sintering temperature on porosity and pore size distribution. The membranes were kept at the desired sintering temperature for about 4 h. This was then followed by slow cooling from sintering temperature to below 100˚C. After sintering, the membranes achieved hard, rigid and porous texture. The membranes were then polished using silicon carbide abrasive paper (C-100 and C-220) to obtain smooth surface. Thereafter, the membranes were sonicated in an ultrasonic bath to remove the loose particles that might have adhered on to the surface of membranes during the polishing step.

2.3. Characterization techniques

Characterization techniques involved the thermo-gravimetric analysis (TGA) of the raw materials paste, structural characterization of membranes by X-ray diffraction (XRD), morphological study by scanning electron microscopy (SEM), porosity determination by gravimetric method, mechanical testing, chemical stability and water permeation. The inorganic mixture was subjected to TGA (EXSTAR TG/DTA 6300) by heating it from room temperature to 1,000˚C at a heating rate of 10˚C/min. The main purpose was to identify the various thermal transformations of the material during sintering process. XRD analysis of membranes was conducted on a diffractometer (D8 Advance, Bruker AXS) using Cu-K_{α} radiation at a wavelength of 1.540598 Å to evaluate the extent of phase transformations. SEM analysis (JSM-6610LV, JEOL) was carried out to analyse the presence of possible defects and estimate the surface pore size distribution. Porosity of the membranes was determined by gravimetric method using water as the wetting liquid. Chemical stability of the membranes was checked by subjecting the membranes to HCl (pH = 1) and NaOH (pH = 13) solutions for seven days.

3. Results and discussion

3.1. Physical observations

Fig. 1 shows a picture of membranes sintered at four different temperatures. A little variation in colour was observed for the membranes sintered at different temperatures. The membranes sintered at 800, 850 and 900˚C were similar in colour, while those sintered at 1,000˚C were light brown in colour. The light yellowish brown colour observed for the membranes sintered at 1,000˚C could be an indication of overheating as the overheated solids, in general, turn to brownish colour [19]. In addition, the membranes sintered at 1,000˚C appeared more rigid and harder than those sintered at other temperatures. This fact is also in accordance with the observations from XRD analysis (Section 3.3) and mechanical testing (Section 3.6).

3.2. Thermo-gravimetric analysis

TGA is an analytical technique used to determine a material's thermal stability by monitoring the weight change that occurs as a specimen is heated. The objective of thermal analysis is to identify temperature regimes where major weight losses (and phase transformations) occur in the membrane and decide upon the minimum sintering temperature. The

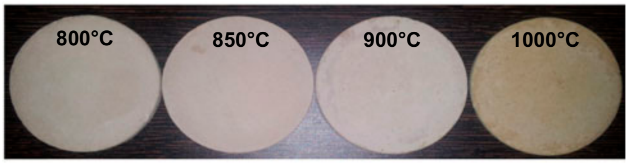

Fig. 1. Picture of membranes sintered at four different temperatures.

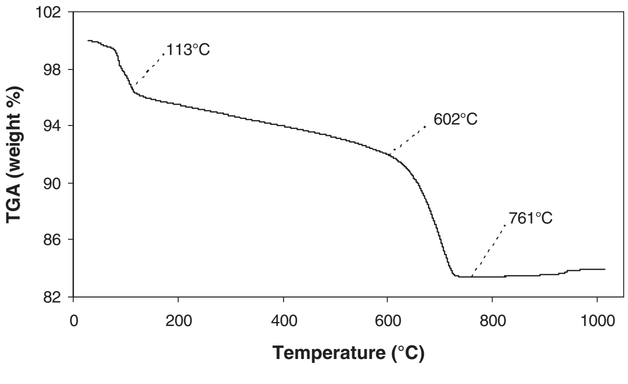

Fig. 2. TGA curve of raw material paste used for membrane fabrication.

TGA shown in Fig. 2 conveys that a highly non-linear variation exists due to the presence of complex phase transformations and interactions. The total weight loss of the sample was observed to be 17%. About 3.45% weight loss was observed below 113℃ due to the removal of weakly bonded water molecules in the sample mixture. The weight loss of sample between 113 and 602℃ was 4.6%, which can be attributed to burning of small impurities and unburned mineral coal powder and also because of evaporation of boric acid whose boiling point is 300℃. The maximum weight loss of about 8.6% occurred in the temperature regime between 602 and 761℃. This is the region where the formation of CO_2 occurred due to the calcination of $CaCO_3$ [18]. Release of CO_2 gas creates vacant spaces and imparts porous structure to the membrane. No weight loss was observed beyond 761℃ as conveyed by the TGA curve and this indicates completion of the calcination process. Therefore, the minimum sintering temperature should be above 761℃. Hence, the sintering temperatures for the fabrication of ceramic membrane using fly ash were so chosen that they were well above this temperature.

3.3. Phase characterization by XRD analysis

XRD (Bruker AXS, D8 Advance) study was done with Cu K_α radiation at a wavelength of 1.540598 Å to identify different phases formed during the sintering process. Fig. 3 shows XRD patterns of five different samples of which one was un-sintered and the other four were sintered at four different temperatures. An observation of peaks and trends in the XRD patterns conveys that the major dominating phase present is anorthite ($CaAl_2Si_2O_8$) while other important phases present are mullite ($2Al_2O_3.SiO_2$), and nacrite and dickite both being the polymorphs of kaolinite ($Al_2Si_2O_5(OH)_4$) having the same molecular formula as kaolinite with different structural arrangements. Apart from these, quartz (SiO_2), iron oxide (Fe_2O_3), aluminium oxide (Al_2O_3) and gehlenite ($Ca_2Al[AlSiO_7]$) were also present in small quantities. A comparison of XRD patterns of different samples indicates the occurrence of continuous phase transformations during the sintering process. Anorthite, which was a major constituent in the other four samples, disappeared in the membrane sintered at 1,000℃ and resulted in the formation of Dmisteinbergite, which is a hexagonal

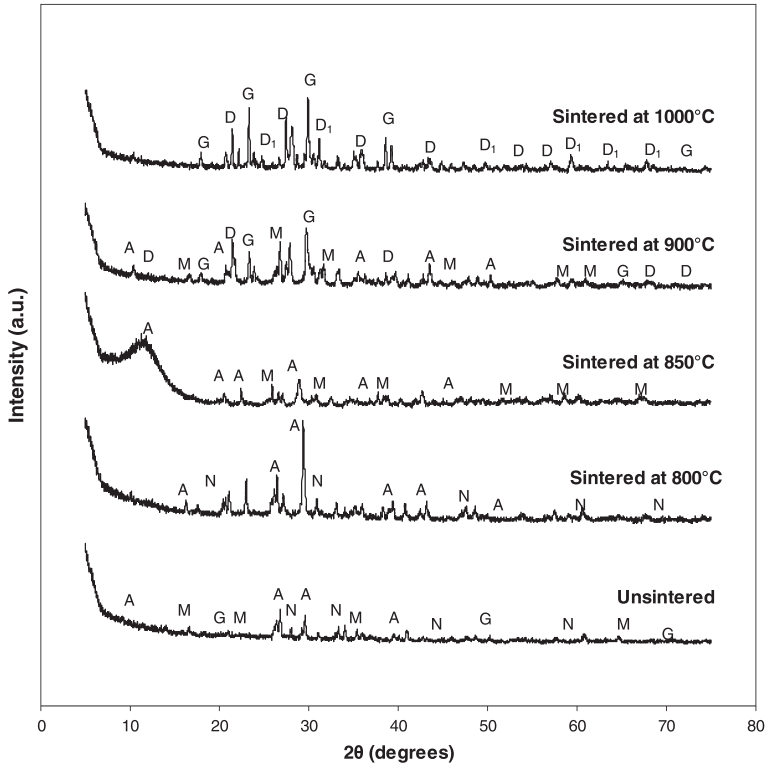

Fig. 3. XRD spectra of membranes sintered at different temperatures. A: Anorthite (JCPDS 41-1486); D: Dickite (JCPDS 10-446); D_1: Dmisteinbergite (JCPDS 31-248); G: Gehlenite (JCPDS 35-755); M: Mullite (JCPDS 15-776); and N: Nacrite (JCPDS 16-606).

polymorph of anorthite. Similarly, other phases also underwent transformations and their content also varied during the sintering process. The hardness value of Dmisteinbergite (present in the membrane sintered at 1,000˚C) is 3 times that of dickite and the hardness value of gehlenite (present in the membrane sintered at 900˚C) is approximately 2.5 times that of nacrite. Therefore, the membranes sintered at higher temperatures (1,000 and 900˚C) were harder than those sintered at lower temperatures (800 and 850˚C).

3.4. Surface morphology and pore size distribution

Fig. 4 illustrates SEM pictures of the membrane sintered at four different temperatures considered in this work. Observation of the SEM pictures indicates that for all sintering temperatures, the membranes did not possess any cracks or surface defects. These micrographs are taken from randomly selected sections of the membrane to ensure that the pore size distribution represents the existing porous texture of the membrane. The SEM image analysis is a simple and reliable method to determine the pore size distribution of ceramic membranes in microfiltration range [20]. Individual pore diameters of about 100 different pores visible in the SEM pictures for each membrane were measured using ImageJ program. Table 2 shows the variation of average pore size of the membrane with sintering temperature. Based on this analysis, it was found that the average pore size decreased with increasing sintering temperature up to 900˚C, while it increased for the membrane sintered at 1,000˚C. This is probably due to the phase transformations observed from XRD analysis.

Fig. 5 presents the surface pore size distribution of the membranes sintered at four different temperatures of 800, 850, 900 and 1,000˚C. For the membranes sintered at 800˚C, about 31% pores have diameters between 0.5 and 1.0 μm, while another 33% pores have diameters between 1.0 and 1.5 μm. Therefore, 64% of the pores have diameters in the range of 0.5–1.5 μm. In case of membranes sintered at 850˚C, about 36% pores have diameters between 0.5 and 1.0 μm while another 28% pores have diameters between 1.0 and 1.5 μm. Therefore, 64% of the pores have diameters in the range of 0.5–1.5 μm. For membranes sintered at 900˚C, about 51% pores have diameters between 0.5 and 1.0 μm while another 27% pores have diameters between 1.0 and 1.5 μm. Therefore, 78% of the pores have diameters in the range of 0.5–1.5 μm. For the membranes sintered at 1,000˚C, pores are widely distributed and about 30% pores have diameters between 1.0 and 1.5 μm. In comparison, the membranes sintered at 900˚C had a narrow (uniform) pore size distribution.

3.5. Porosity results

The porosity of the membranes was determined by the gravimetric method [20] using water as the wetting liquid. To take into account the variation in the dimensions of membranes due to polishing, their thickness and diameter were measured at different

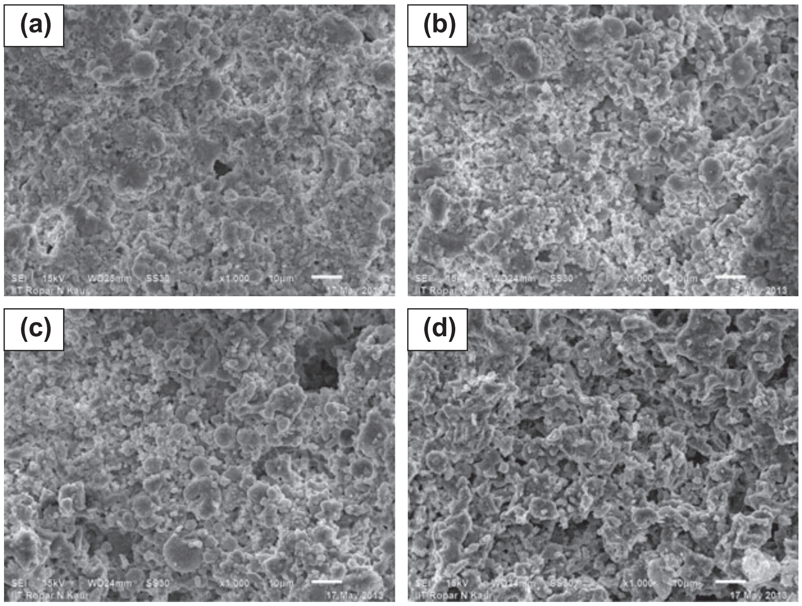

Fig. 4. SEM images of membranes sintered at different temperatures: (a) 800˚C; (b) 850˚C; (c) 900˚C; and (d) 1,000˚C.

Table 2
Variation of average pore size of the membranes with sintering temperature

Sintering temperature (˚C)	Minimum pore size (μm)	Maximum pore size (μm)	Average pore size (μm)
800	0.271	5.602	1.524
850	0.336	4.891	1.458
900	0.399	13.689	1.202
1,000	0.636	9.634	2.301

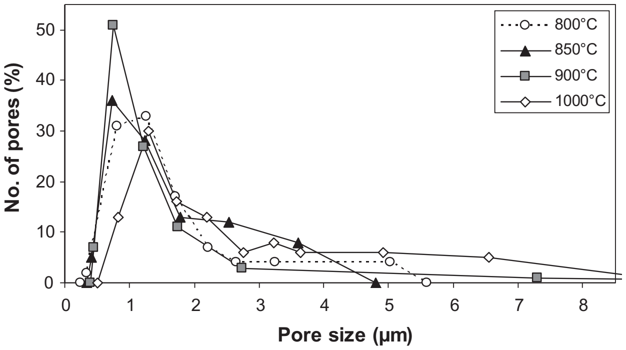

Fig. 5. Surface pore size distribution of membranes sintered at four different temperatures.

locations and the average values were used for calculating the membrane porosity. The percentage porosity was calculated using the relation given in Eq. (1):

$$\text{Porosity}\,(\%) = \frac{\text{Volume of pores}}{\text{Total volume}} \times 100 \tag{1}$$

The variation of membrane porosity with sintering temperature is shown in Fig. 6. With the increase in sintering temperature from 800 to 900˚C, the porosity of the membranes decreased from 38.1 to 34.8% and the membrane became more compact due to the densification of the solid structure. However, the membranes sintered at 1,000˚C showed a sharp increase in porosity to a value of 39.7% due to the presence of Dmisteinbergite which resulted in the formation of larger pores corroborating the observation of larger average pore size.

3.6. Mechanical strength

The mechanical strength of the membranes is determined using the three-point bending strength method. Fig. 7 shows the variation of flexural strength of the membranes with sintering temperature. From this figure, it is clear that the flexural strength increases with increasing sintering temperature. The increase in mechanical strength is due to the formation of Dmisteinbergite and Gehlenite at higher sintering temperatures (observed from XRD analysis). These findings are in accordance with the physical observations discussed in Section 3.1. The observed trend is in good agreement with that reported in literature for kaolin-based membranes [18] and the results obtained indicate that the membranes prepared using fly ash have better mechanical strength (8–20 MPa) than those made of kaolin (3–8 MPa).

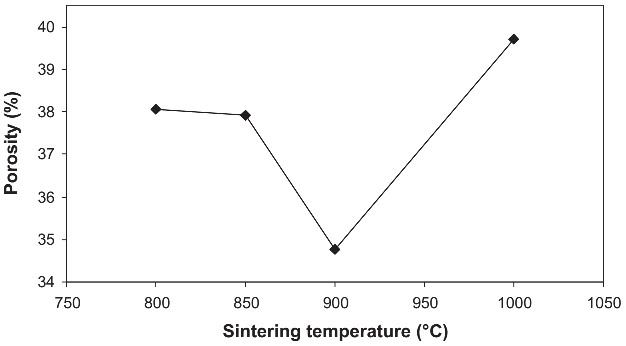

Fig. 6. Variation of porosity with sintering temperature.

3.7. Chemical stability

The membranes sintered at four different temperature were kept in HCl (pH = 1) and NaOH (pH = 13) solutions for seven days to check their chemical stability. The difference in the dry weights of membranes before and after acid or base treatment gives the weight loss. Fig. 8 shows percentage weight loss of the membranes sintered at various tempera-

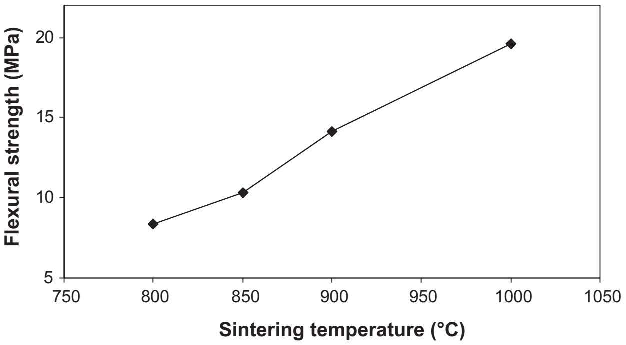

Fig. 7. Variation of flexural strength with sintering temperature.

tures when subjected to acid and base treatment. The weight loss of all membranes in both acid and base solutions was found to be less than 2%. Based on the experimental results, it can be inferred that the membranes had good chemical stability against acidic as well as basic conditions at all sintering temperatures. As expected, the membranes sintered at 1,000˚C performed slightly better than the other membranes sintered at 800, 850 and 900˚C under both acidic and basic conditions.

3.8. Water permeation test

The prepared membranes were subjected to water permeation test to determine water permeability of the membranes using a batch permeation cell (shown in Fig. 9) with an effective filtration area of 28.2 cm^2. The membrane was fixed to the base of the permeation cell using an epoxy resin. The cell was filled by distilled water pressurized using an air compressor. Each membrane was compacted for about 2 h until the attainment of a steady flux at an absolute pressure of 515 kPa and the permeate flux was measured by varying the transmembrane pressure difference between 0 and 345 kPa. The hydraulic permeability values of the membranes sintered at 800, 850, 900 and 1,000˚C, respectively, were 2,304, 2,158, 1,234 and 5,566 L/(m^2 h bar). Among all the membranes, the lowest value of water permeability was observed for the membrane sintered at 900˚C owing to its lowest average pore size (1.2 μm) and porosity (34.76%).

3.9. Treatment of oil-in-water emulsion

Synthetic solution (50 mg/L) of oil-in-water emulsion was prepared and sonicated in an ultrasonic

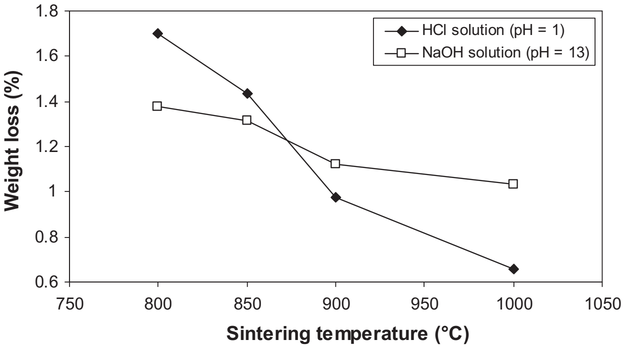

Fig. 8. Weight loss (%) of membranes in acid (HCl) and base (NaOH) solutions.

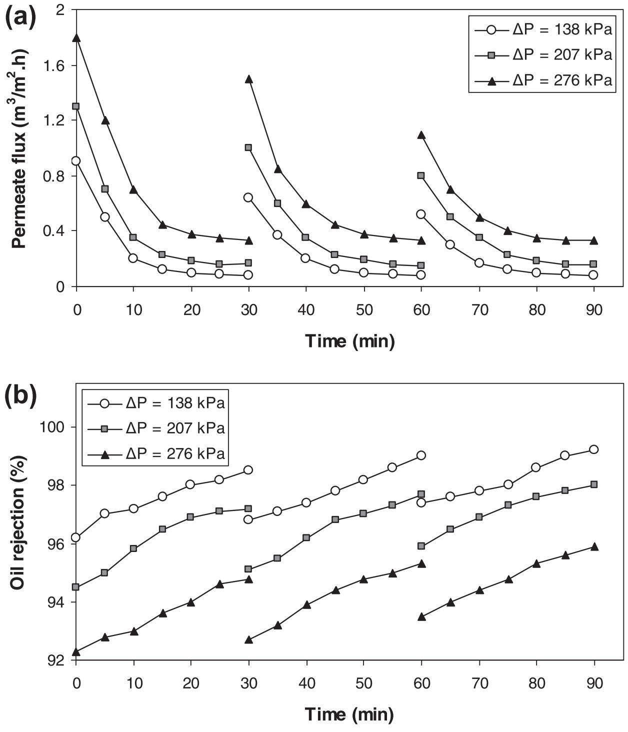

Fig. 10. Microfiltration of oil-in-water emulsion: (a) permeate flux; and (b) rejection profiles.

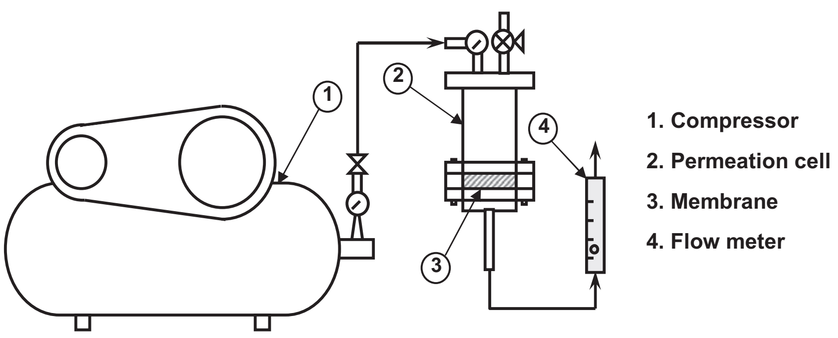

Fig. 9. Schematic diagram of set-up used for water permeation and microfiltration experiments.

Table 3
Cost comparison of various raw materials used in membrane fabrication

Material	Unit price ($/kg)	Composition on dry basis (wt.%)		
		Literature [20]	Literature [21]	This work
Fly ash	0	0	0	65
Kaolin	7	40	40	0
Quartz	64	15	15	0
Feldspar	88	15	0	0
Pyrophyllite	76	10	0	0
Calcium carbonate	4	0	25	20
Sodium carbonate	5	10	10	10
Boric acid	6	5	5	2.5
Sodium metasilicate	10	5	5	2.5
Cost of membrane material ($/kg)		34.5	14.7	1.7
Cost of membrane material ($/m^2)		351.6	149.8	17.3
Average pore size (μm)		0.3	0.7	1.2

bath for 6 h. Batch microfiltration experiments were carried out at three different transmembrane pressure differences (ΔP) of 138, 207 and 276 kPa. The membrane sintered at 900°C was chosen for the separation of oil-in-water emulsion because of its lowest average pore size (1.2 μm) and uniform pore size distribution. The concentrations of oil in feed and permeate were determined at a wavelength ($\lambda_{\max}$) of 235 nm using a UV-vis spectrophotometer. The permeate was collected into a volumetric flask at uniform time intervals. Fig. 10 presents the permeate flux and oil rejection profiles at different transmembrane pressure differences. The membrane was subjected to manual cleaning and back flushing at a transmembrane pressure difference (ΔP) of 69 kPa with a surfactant solution followed by distilled water after every 30 min of the microfiltration cycle. The permeate flux decreased with time due to the resistance from cake formation and/or pore blockage. On the other hand, oil rejection increased slightly with time as a result of decrease in average pore size due to the presence of oil layer on the membrane surface and in the interior of the pores. The flux values obtained in this work (0.08–0.33 m^3/m^2 h) are better than those reported (0.03–0.10 m^3/m^2 h) by Nandi et al. [12] using kaolin-based membranes of pore size 0.55 μm. The maximum oil rejection of 99.2% was obtained at a transmembrane pressure difference (ΔP) of 138 kPa. Therefore, the prepared fly ash-based low-cost ceramic membranes are useful for microfiltration applications.

3.10. Cost analysis

The retail prices of various raw materials used in this work as well as others are shown in Table 3. The prices shown in the table are approximate and were taken from the price tags of the retail packs and company catalogues. The average pore sizes of membranes sintered at the same temperature (900°C) are also shown in this table. As shown in the table, the cost of raw materials mixture used in this work is only 5% of the membrane having an average pore diameter of 0.3 μm [20] and 12% of the membrane having the average pore size of 0.7 μm [21]. However, the cost of heating and sintering is the same for all membranes fired at the same temperature and a reduction in raw material cost contributes directly to the lowering of membrane cost. Therefore, the fly ash-based microfiltration membranes prepared in this work are cost effective and can be designated as low-cost ceramic membranes.

4. Conclusions

This work is unique to use fly ash with inorganic precursors as the earlier studies reported so far used fly ash in combination with organic additives such as starch to prepare membranes. This study showed that fly ash combined with inorganic precursors such as calcium carbonate is a good candidate to fabricate low-cost microfiltration membranes without any defects. Based on the TGA analysis, it can be inferred that the sintering temperature of membranes should be above 761°C. The membranes fabricated at four different sintering temperatures showed porosity in the range of 34.75–39.72% which is considered to be reasonably good. The average pore size of the sintered membranes varied in the range of 1.2–2.3 μm. The fabricated membranes showed very good mechanical strength and excellent chemical resistance exhibiting less than 2% weight loss in both acid and base solutions. The pure water permeability of the membranes varied from 1,234 to 5,566 L/(m^2 h bar). In comparison with other membranes, the membranes sintered at 900℃ had a uniform pore size distribution with an average pore diameter of 1.2 μm. Flux decline profiles for the separation of oil-in-water were obtained and the maximum oil rejection of 99.2% was obtained for the membrane sintered at 900℃ which indicates that the membranes made of fly ash are useful for microfiltration applications. In addition to the inherent advantages such as abundant availability of fly ash and low-cost formulation, the fly ash-based membranes prepared in this work showed superior mechanical strength and better corrosion resistance along with good hydraulic permeability and high flux properties. This study has paved a way for further research on the development of low-cost ceramic membranes suitable for a wide variety of applications using fly ash which is considered as a potential contaminant in many parts of the world.

References

[1] S. Sourirajan, Reverse Osmosis. Logos Press, London, 1970.

[2] Y. Yoshino, T. Suzuki, B.N. Nair, H. Taguchi, N. Itoh, Development of tubular substrates, silica based membranes and membrane modules for hydrogen separation at high temperature, J. Membr. Sci. 267 (2005) 8–17.

[3] Y.H. Wang, T.F. Tian, X.Q. Liu, G.Y. Meng, Titania membrane preparation with chemical stability for very hash environments applications, J. Membr. Sci. 280 (2006) 261–269.

[4] K.A. DeFriend, M.R. Wiesner, A.R. Barron, Alumina and aluminate ultrafiltration membranes derived from alumina nanoparticles, J. Membr. Sci. 224 (2003) 11–28.

[5] T. Tsuru, Inorganic porous membranes for liquid phase separation, Sep. Purif. Rev. 30 (2001) 191–220.

[6] C. Falamaki, M.S. Afarani, A. Aghaie, Initial sintering stage pore growth mechanism applied to the manufacture of ceramic membrane supports, J. Eur. Ceram. Soc. 24 (2004) 2285–2292.

[7] S. Masmoudi, A. Larbot, H.E. Feki, R.B. Amar, Elaboration and characterisation of apatite based mineral supports for microfiltration and ultrafiltration membranes, Ceram. Int. 33 (2007) 337–344.

[8] Y. Dong, X. Liu, Q. Ma, G. Meng, Preparation of cordierite-based porous ceramic micro-filtration membranes using waste fly ash as the main raw materials, J. Membr. Sci. 285 (2006) 173–181.

[9] S. Khemakhem, R.B. Amara, Purification of industrial effluent by microfiltration and ultrafiltration ceramic membranes: Comparative study between commercial and elaborated Tunisian clay membranes, Desalin. Water Treat. 39 (2012) 182–189.

[10] S. Jana, M.K. Purkait, K. Mohanty, Polymer enhanced ultrafiltration of mercury using chitosan impregnated ceramic membrane, Desalin. Water Treat. 37 (2012) 321–330.

[11] N.E. Baraka, N. Saffaj, R. Mamouni, A. Laknifli, S.A. Younssi, A. Albizane, M.E. Haddad, Elaboration of a new flat membrane support from Moroccan clay, Desalin. Water Treat. (in press), doi: http://10.1080/19443994.2013.797542.

[12] B.K. Nandi, R. Uppaluri, M.K. Purkait, Microfiltration of stable oil-in-water emulsions using kaolin based ceramic membrane and evaluation of fouling mechanism, Desalin. Water Treat. 22 (2010) 133–145.

[13] A. Potdar, A. Shukla, A. Kumar, Effect of gas phase modification of analcime zeolite composite membrane on separation of surfactant by ultrafiltration, J. Membr. Sci. 210 (2002) 209–225.

[14] C. Neelakandan, G. Pugazhenthi, A. Kumar, Preparation of NOx modified PMMA–EGDM composite membrane for the recovery of chromium (VI), Eur. Polym. J. 39 (2003) 2383–2391.

[15] S. Jana, M.K. Purkait, K. Mohanty, Preparation and characterization of low-cost ceramic microfiltration membranes for the removal of chromate from aqueous solutions, Appl. Clay Sci. 47 (2010) 317–324.

[16] V.K. Bulasara, R. Uppaluri, M.K. Purkait, Manufacture of nickel-ceramic composite membranes in agitated electroless plating baths, Mater. Manuf. Process. 26 (2011) 862–867.

[17] I. Jedidi, S. Khemakhem, S. Saïdi, A. Larbot, N.E. Ammar, A. Fourati, A. Charfi, A.B. Salah, R.B. Amar, Preparation of a new ceramic microfiltration membrane from mineral coal fly ash: Application to the treatment of the textile dying effluents, Powder Technol. 208 (2011) 427–432.

[18] B.K. Nandi, R. Uppaluri, M.K. Purkait, Preparation and characterization of low cost ceramic membranes for micro-filtration applications, Appl. Clay Sci. 42 (2008) 102–110.

[19] J.S. Reed, Principles of Ceramics Processing, 2nd ed. John Wiley & Sons, New York, NY, 1995.

[20] V.K. Bulasara, H. Thakuria, R. Uppaluri, M.K. Purkait, Effect of process parameters on electroless plating and nickel-ceramic composite membrane characteristics. Desalination 268 (2011) 195–203.

[21] V.K. Bulasara, O. Chandrashekar, R. Uppaluri, Effect of surface roughness and mass transfer enhancement on the performance characteristics of nickel-hypophosphite electroless plating baths for metal–ceramic composite membrane fabrication, Chem. Eng. Res. Des. 89 (2011) 2485–2494.